

DYNAMIC GENERATION OF MULTI LLM AGENTS COMMUNICATION TOPOLOGIES WITH GRAPH DIFFUSION MODELS

Eric H. Jiang^{1*}, Guancheng Wan^{1*}, Sophia Yin^{1*}, Mengting Li^{1*}, Yuchen Wu², Xiao Liang¹, Xinfeng Li³, Yizhou Sun¹, Wei Wang¹, Kai-Wei Chang¹, Ying Nian Wu¹

¹ University of California, Los Angeles ² University of Washington ³ Nanyang Technological University

ABSTRACT

The efficiency of multi-agent systems driven by large language models (LLMs) largely hinges on their communication topology. However, designing an optimal topology is a non-trivial challenge, as it requires balancing competing objectives such as task performance, communication cost, and robustness. Existing frameworks often rely on static or hand-crafted topologies, which inherently fail to adapt to diverse task requirements, leading to either excessive token consumption for simple problems or performance bottlenecks for complex ones. To address this challenge, we introduce a novel generative framework called *Guided Topology Diffusion (GTD)*. Inspired by conditional discrete graph diffusion models, GTD formulates topology synthesis as an iterative construction process. At each step, the generation is steered by a lightweight proxy model that predicts multi-objective rewards (e.g., accuracy, utility, cost), enabling real-time, gradient-free optimization towards task-adaptive topologies. This iterative, guided synthesis process distinguishes GTD from single-step generative frameworks, enabling it to better navigate complex design trade-offs. We validated GTD across multiple benchmarks, and experiments show that this framework can generate highly task-adaptive, sparse, and efficient communication topologies, significantly outperforming existing methods in LLM agent collaboration. Our code is available at: https://github.com/ericjiang18/diffusion_agent

1 INTRODUCTION

Large language model (LLM) driven multi-agent systems (MAS) increasingly rely on structured communication to solve complex tasks, yet a core open problem is how to *dynamically* design the communication topology for a given task and team. In practice, many systems still adopt hand-crafted or heuristic patterns (e.g., chain, star, or fully connected graphs) or workflow templates and role play frameworks (Wu et al., 2023; Hong et al., 2023; Li et al., 2023; Chen et al., 2023b). Such static or rule-based designs struggle to adapt to the intrinsic complexity of the task, the composition of skills required, or real-time progress. Classical MAS theory already shows that performance and robustness depend critically on the underlying graph (e.g., consensus rates and failure modes are tied to connectivity and spectral properties) (Zhu, 2006; Chen et al., 2013). The mismatch manifests in practice: a simple Q&A may need only a short linear exchange, whereas software development benefits from a richer collaboration network with project managers, programmers, and testers (Hong et al., 2023). Using one pattern for all tasks either inflates token/communication overhead for simple problems or creates bottlenecks for complex ones (Zhang et al., 2024). Recent efforts begin to *optimize* or *search* topologies, but typically emphasize end utility (accuracy) while underweighting other crucial dimensions such as communication cost (token consumption), robustness to agent failures/attacks, and sparsity/efficiency (Zhang et al., 2025a; Sun et al., 2025; Zhou et al., 2025; Hu et al., 2024b; Shang et al., 2024; Chen et al., 2025). Furthermore, their reliance on single-step generation mechanisms, such as variational auto-encoders, can limit the fine-grained exploration of the

*Equal contribution.

multi-objective design space. A principled topology designer should therefore seek Pareto-optimal trade-offs in a multi-objective space (Zhang et al., 2025c).

However, while these adaptive methods represent a significant step forward, they face two fundamental limitations. (1) First, their generative process often relies on single-step models like variational auto-encoders, which can struggle to capture the complex, long-range dependencies inherent in optimal communication structures. This may constrain the search space to topologies that are plausible but not truly Pareto-optimal. (2) Second, their optimization is often coarse-grained, applying reward signals only after a complete topology has been generated. Such post-hoc guidance makes it difficult to navigate the intricate trade-offs between competing objectives like task utility, token cost, and robustness in a fine-grained manner. The core research problem, therefore, is to develop a framework that can powerfully yet precisely construct topologies by integrating multi-objective guidance directly into each step of the generative process.

To address this challenge, we reframe topology synthesis as a guided, iterative construction process. We introduce **Guided Topology Diffusion (GTD)**, a framework that casts topology generation as a conditional discrete graph diffusion process, drawing on recent advances in generative modeling (Ho et al., 2020; Song & Ermon, 2021; Ho & Salimans, 2021; Vignac et al., 2023). By starting from a noisy graph and progressively denoising it, GTD leverages the strong generative capabilities of diffusion models to explore a richer design space. Crucially, we inject multi-objective guidance at each step of this reverse process. We achieve this by coupling the generator with a lightweight *proxy reward model* and performing *zeroth-order* (gradient-free) optimization during sampling, a scheme inspired by reward-modeling and gradient-free optimization practice (Nesterov & Spokoiny, 2017; Liu et al., 2018; Ouyang et al., 2022; Li et al., 2025a;b; Jiang et al., 2025; Liang et al., 2025b; Wen et al., 2025; Liang et al., 2025a). This allows GTD to steer the generation trajectory in real-time, effectively balancing task utility, communication cost, and robustness to produce highly optimized, task-specific topologies.

In summary, our contributions are threefold:

- ❶ **Problem Level:** We propose GTD, a novel conditional discrete graph diffusion framework for dynamically generating multi-agent communication topologies.
- ❷ **Algorithm Level:** We design and implement a proxy model-based zeroth-order optimization guidance algorithm, which effectively optimizes non-differentiable, high-cost external objectives during the diffusion process.
- ❸ **Framework Level:** We construct a complete end-to-end solution that integrates advanced semantic feature encoding, conditional graph diffusion generation, and multidimensional protocol-based dynamic guidance, providing a new paradigm for solving such complex graph generation problems.

2 RELATED WORK

2.1 COMMUNICATION TOPOLOGIES IN MULTI-AGENT SYSTEMS

Classical MAS research establishes that communication topology strongly shapes global behavior: consensus speed and robustness depend on connectivity and spectral properties, while practical systems emphasize scalability and modularity over automatic topology synthesis (Zhu, 2006; 2003; Chen et al., 2013;

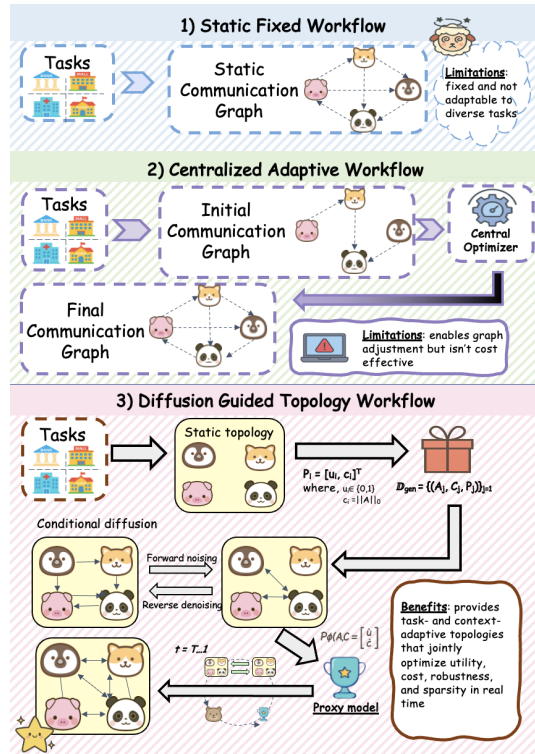


Figure 1: Comparison of Multi-Agent System (MAS) communication topology design workflows. (1) **Static Fixed Workflow**, (2) **Centralized Adaptive Workflow**, (3) **Diffusion Guided Topology Workflow (Ours)**. Our proposed method provides task- and context-adaptive topologies by using a conditional diffusion process guided by a proxy model to jointly optimize for utility, cost, robustness, and sparsity.

Helsingør et al., 2004; Ayal a, 2025). Analyses of star-like networks quantify the trade-off between rapid information propagation and single-point-of-failure risk (Chowdhury & Khalil, 2017; Gong et al., 2015). Learning within fixed or topology-constrained settings has been explored via cooperative RL (Xiao & Tan, 2013). Beyond LLM agents, multi-objective workflow schedulers and structural/topology optimization study Pareto fronts (e.g., makespan, cost, reliability), motivating designs that jointly balance accuracy, sparsity, and resilience rather than optimizing a single metric (Zhang et al., 2025c; str, 2023; Zhang et al., 2025e; Wan et al., 2025).

2.2 DYNAMIC TOPOLOGY GENERATION FOR LLM AGENTS

In LLM-based MAS, recent work reduces redundant exchanges and token budgets without changing the assumed graph class, or learns path-like collaboration schedules via next-agent prediction; others co-optimize prompts and wiring yet rely on task-agnostic heuristics (Zhang et al., 2024; Yang et al., 2025; Zhou et al., 2025). Closest to our setting are methods that *learn* the communication graph: G-Designer uses GNNs to design task-aware topologies (Zhang et al., 2025a), and Assemble-Your-Crew performs autoregressive graph generation conditioned on task context (Sun et al., 2025). Other approaches such as ExpoComm (Li et al., 2025c), DACOM (Yuan et al., 2023), and MADRL (Zhu et al., 2025) address scalability and latency in decentralized settings.

2.3 GRAPH DIFFUSION MODELS FOR SYNTHESIS

Recent advances in generative modeling have introduced powerful techniques for graph synthesis. Conditional graph diffusion models, in particular, have shown promise in various domains, inspiring our generative backbone (Xu et al., 2024; Vignac et al., 2023; Madeira et al., 2024). Our work also draws inspiration from other generative approaches for graphs like GCPN (You et al., 2018) and various communication-efficient paradigms (Lo et al., 2024; Du et al., 2024; Ding et al., 2024; Hu et al., 2024a; Zhao et al., 2024; Ji et al., 2025). Distinctly, our **GTD** is the first to integrate a fine-grained, proxy-guided zeroth-order optimization step directly into the sampling phase of a discrete graph diffusion process. This allows GTD to directly steer generation toward multi-objective optima (e.g. utility, token cost, sparsity, and robustness) without requiring differentiable or low-cost evaluators.

3 PRELIMINARIES

In this section, we formalize the problem of topology generation and describe the underlying principles of graph diffusion models, pinpointing the limitations that motivate our proposed method.

3.1 FORMALIZING TOPOLOGY GENERATION AS A CONDITIONAL GENERATIVE PROBLEM

The design of an optimal communication topology for a Multi-Agent System (MAS) can be framed as a conditional graph generation problem. Given a set of N agents, their communication structure is represented by a directed graph $G = (V, E)$, where $|V| = N$. This graph is fully described by its adjacency matrix $A \in \{0, 1\}^{N \times N}$, where $A_{ij} = 1$ signifies that agent i can send a message to agent j .

Optimization Objective. For a given task query q and a set of available agents, which together form a task-specific condition vector C , the goal is to discover an optimal adjacency matrix A^* that maximizes a composite reward function $\mathcal{R}(A, C)$. This function evaluates the quality of a topology based on multiple criteria:

$$\max_A \mathcal{R}(A, C) = f(\text{Utility}(A, C), \text{Cost}(A, C), \text{Sparsity}(A), \dots) \quad (1)$$

Here, **Utility** measures task success (e.g., accuracy), **Cost** quantifies token consumption or communication overhead, and **Sparsity** encourages efficiency. Evaluating $\mathcal{R}(A, C)$ is computationally expensive, as it requires executing a full, costly multi-agent simulation for each candidate graph A .

3.2 DENOISING DIFFUSION MODELS FOR GRAPH GENERATION

Denoising diffusion models are a class of powerful generative models that learn to synthesize data by reversing a gradual noising process. We adapt this paradigm for discrete graph structures.

Forward Diffusion Process. The forward process, $q(A_t|A_0)$, systematically corrupts an initial graph A_0 by adding noise over T discrete timesteps. To operate in a continuous space, we first scale the adjacency matrix entries from $\{0, 1\}$ to $\{-1, 1\}$. The forward process is then defined as a variance-preserving schedule that adds Gaussian noise:

$$q(A_t|A_0) = \mathcal{N}(A_t; \sqrt{\bar{\alpha}_t}A_0, (1 - \bar{\alpha}_t)I) \quad (2)$$

where $\{\beta_t\}_{t=1}^T$ is a predefined noise schedule, $\alpha_t = 1 - \beta_t$, and $\bar{\alpha}_t = \prod_{s=1}^t \alpha_s$. As $t \rightarrow T$, the distribution of A_T converges to a standard isotropic Gaussian distribution, $\mathcal{N}(0, I)$.

Learned Reverse Process. The generative model learns the reverse process, $p_\theta(A_{t-1}|A_t, C)$, to denoise a noisy graph A_t and recover a cleaner version A_{t-1} , conditioned on the task context C . This is parameterized by a denoising network $\mathcal{G}_\theta(A_t, C, t)$, which is trained to predict the original clean graph A_0 from its noisy counterpart A_t . The training objective for \mathcal{G}_θ is to minimize the reconstruction error over a dataset of high-performing graphs:

$$\mathcal{L}_\theta = \mathbb{E}_{t, A_0, C, \epsilon} \left[\|A_0 - \mathcal{G}_\theta(\sqrt{\bar{\alpha}_t}A_0 + \sqrt{1 - \bar{\alpha}_t}\epsilon, C, t)\|^2 \right] \quad (3)$$

where $\epsilon \sim \mathcal{N}(0, I)$. Once trained, we can generate a new graph by sampling $A_T \sim \mathcal{N}(0, I)$ and iteratively applying the denoising network to obtain A_0 .

3.3 THE CHALLENGE: GUIDING GENERATION WITH A BLACK-BOX OBJECTIVE

A standard conditional diffusion model can generate topologies that are statistically similar to those in the training data, but it cannot explicitly optimize for the external reward function $\mathcal{R}(A, C)$ during generation. Steering the denoising process toward high-reward structures presents two major obstacles. First, the true reward function \mathcal{R} is too slow to be used for guidance within the iterative sampling loop, a challenge of **high-cost evaluation**. Second, the reward is a **non-differentiable “black-box” objective**; the output of the denoising network, \mathcal{G}_θ , is a continuous prediction that must be converted into a discrete graph A before evaluation, and this sampling step breaks the end-to-end differentiability, rendering gradient-based guidance techniques inapplicable. To overcome these challenges, we reframe the problem by introducing a method for efficient, gradient-free guidance. This is achieved by first training a lightweight **surrogate model (or proxy)** that accurately approximates the expensive reward \mathcal{R} and then using this proxy during inference to guide the diffusion sampling process with a **Zeroth-Order (ZO) optimization** scheme. This approach transforms the generation process from a simple denoising task into a guided synthesis, allowing us to directly optimize for task-specific, multi-objective rewards without requiring differentiability.

4 METHODOLOGY

Our framework, **Guided Topology Diffusion (GTD)**, learns to generate optimal communication topologies for Multi-Agent System (MAS). GTD comprises two core components: (1) a **surrogate reward model**, \mathcal{P}_ϕ , that approximates the expensive simulation outcomes, and (2) a **conditional diffusion generator**, \mathcal{G}_θ , that learns the distribution of high-performing graph structures. We first train these components on a pre-computed dataset and then integrate them for a novel, guided synthesis process at inference time.

4.1 SURROGATE REWARD MODEL

To circumvent the computational cost of direct simulation, we first train a surrogate model \mathcal{P}_ϕ to predict the performance of a given topology. This model maps a graph-condition pair (A, C) to a performance vector $[\hat{u}, \hat{c}]^T$, representing the predicted task utility and communication cost, respectively.

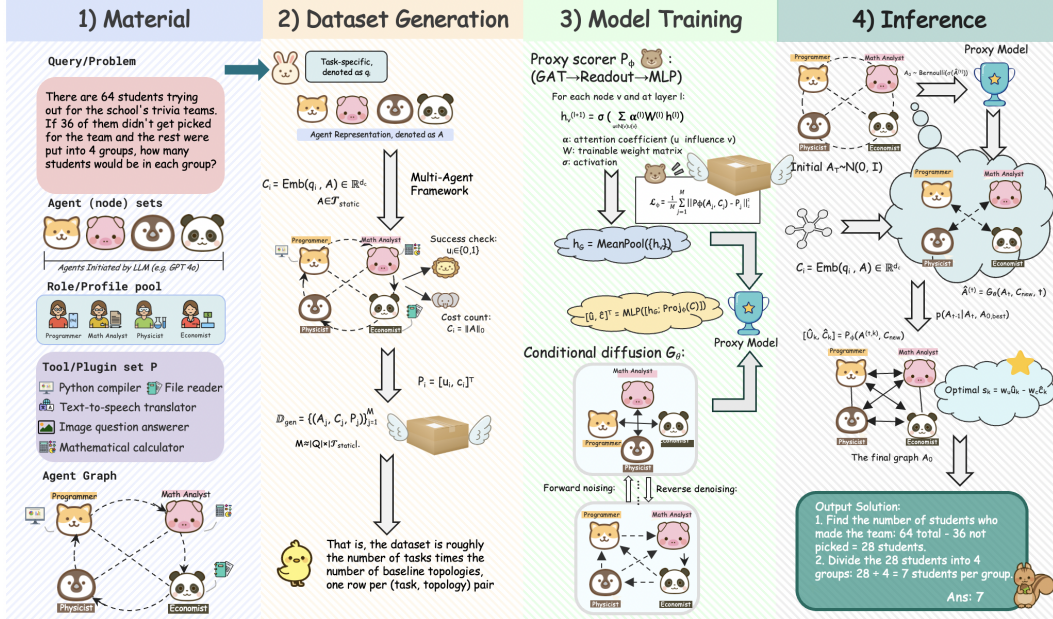


Figure 2: **The Guided Topology Diffusion (GTD) framework workflow**, divided into four main stages. **1) Material:** The process begins with task-specific inputs, including the query, available agents, and tools. **2) Dataset Generation:** A multi-agent framework simulates various baseline topologies to generate a foundational dataset linking topologies to performance outcomes (e.g., utility and cost). **3) Model Training:** The generated dataset is used to train two core components: a lightweight proxy scorer (P_ϕ) to predict topology performance and a conditional graph diffusion generator (G_θ) to learn the structure of high-performing graphs. **4) Inference:** For a new task, the framework uses the trained models to iteratively denoise a random graph, with the proxy scorer guiding each step to synthesize a final, task-optimized topology.

Architecture. The surrogate \mathcal{P}_ϕ is implemented as a Graph Neural Network (GNN). Specifically, we employ a series of Graph Attention (GAT) layers to learn expressive node representations. The update rule for a node v 's hidden state \mathbf{h}_v from layer (l) to $(l+1)$ is given by:

$$\mathbf{h}_v^{(l+1)} = \sigma \left(\sum_{u \in \mathcal{N}(v) \cup \{v\}} \alpha_{vu}^{(l)} \mathbf{W}^{(l)} \mathbf{h}_u^{(l)} \right) \quad (4)$$

where $\alpha_{vu}^{(l)}$ are the learned attention coefficients between nodes v and u . The final node embeddings are aggregated via mean pooling to produce a graph-level representation \mathbf{h}_G . This is concatenated with the projected task condition vector C and processed by a multi-layer perceptron (MLP) to yield the final prediction: $[\hat{u}, \hat{c}]^T = \text{MLP}_\phi([\mathbf{h}_G; \text{Proj}_\phi(C)])$.

Training. We first generate a foundational dataset $\mathcal{D}_{\text{gen}} = \{(A_j, C_j, P_j)\}_{j=1}^M$ by running simulations for a diverse set of baseline topologies across various tasks. The model \mathcal{P}_ϕ is then trained to minimize the Mean Squared Error (MSE) loss between its predictions and the ground-truth performance vectors from simulation:

$$\mathcal{L}_\phi = \frac{1}{M} \sum_{j=1}^M \|\mathcal{P}_\phi(A_j, C_j) - P_j\|_2^2 \quad (5)$$

4.2 CONDITIONAL GRAPH DIFFUSION GENERATOR

The core of our generative framework is a conditional diffusion model, \mathcal{G}_θ , designed to learn the distribution of high-quality topologies, $p_\theta(A|C)$. Here, in Figure 3, we provide a visual contrast between common static topologies and the sparse, adaptive structures that our generator is designed to create. This distinction highlights the framework's goal: to move beyond one-size-fits-all patterns towards topologies optimized for the specific demands of a given task. We model the adjacency matrix $A \in \{0, 1\}^{N \times N}$ by scaling its values to $\{-1, 1\}$ and performing diffusion in a continuous space.

Diffusion Process. We utilize a variance-preserving forward process $q(A_t|A_0)$ that gradually adds Gaussian noise to an initial graph A_0 over T timesteps:

$$q(A_t|A_0) = \mathcal{N}(A_t; \sqrt{\bar{\alpha}_t}A_0, (1 - \bar{\alpha}_t)\mathbf{I}) \quad (6)$$

where $\{\beta_t\}_{t=1}^T$ is a fixed variance schedule and $\bar{\alpha}_t = \prod_{s=1}^t (1 - \beta_s)$. The objective is to learn the reverse process $p_\theta(A_{t-1}|A_t, C)$ to denoise a noisy graph A_t back towards a clean, high-performance graph, conditioned on the task vector C .

Denoising Network and Training. We parameterize the reverse process with a denoising network $\mathcal{G}_\theta(A_t, C, t)$, which is implemented as a **Graph Transformer**. This architecture’s global attention mechanism is well-suited for capturing long-range dependencies inherent in graph topology optimization. The network is trained to predict the original graph A_0 from its noised version A_t . To focus the model on generating effective topologies, we train it exclusively on a high-performance subset $\mathcal{D}_{\text{hq}} \subset \mathcal{D}_{\text{gen}}$, where graphs exceed a certain performance threshold. The training objective is to minimize the binary cross-entropy (BCE) loss:

$$\mathcal{L}_\theta = \mathbb{E}_{t, A_0 \sim p_{\text{hq}}, C, \epsilon} [\text{BCE}(\mathcal{G}_\theta(\sqrt{\bar{\alpha}_t}A_0 + \sqrt{1 - \bar{\alpha}_t}\epsilon, C, t), A_0)] \quad (7)$$

where $\epsilon \sim \mathcal{N}(0, \mathbf{I})$. This objective serves as a practical surrogate for maximizing the true Evidence Lower Bound, a connection we formalize in Appendix C (see Theorem C.3).

4.3 PROXY-GUIDED TOPOLOGY SYNTHESIS

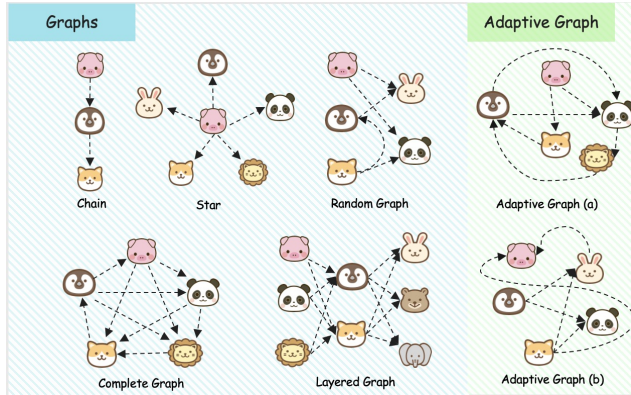


Figure 3: **An illustration of different multi-agent communication topologies.** The left panel shows examples of common static or heuristic graphs, such as **Chain**, **Star**, **Complete**, **Layered**, and **Random** graphs. The right panel shows examples of **Adaptive Graphs**, which represent the sparse, task-specific topologies that the GTD framework is designed to generate dynamically.

select the one that maximizes our composite reward objective:

$$A_{0,\text{best}}^{(t)} = \arg \max_{A_{0,k}^{(t)}} (w_u \cdot \hat{u}_k - w_c \cdot \hat{c}_k) \quad \text{s.t.} \quad [\hat{u}_k, \hat{c}_k]^T = \mathcal{P}_{\phi^*}(A_{0,k}^{(t)}, C_{\text{new}}) \quad (8)$$

This best-ranked candidate, $A_{0,\text{best}}^{(t)}$, is then used in place of the original prediction $\hat{A}_0^{(t)}$ to compute the posterior distribution $q(A_{t-1}|A_t, A_{0,\text{best}}^{(t)})$ for sampling the next state A_{t-1} . This procedure directly injects task-specific performance objectives into the generative trajectory, guiding the synthesis towards topologies that are optimized for the given task. The effectiveness of this guidance is directly tied to the fidelity of the surrogate model \mathcal{P}_{ϕ^*} . In Appendix C, we formally bound the performance gap of the resulting topology as a function of the surrogate’s approximation error (Theorem C.5).

At inference, we synthesize a topology for a novel task condition C_{new} by steering the diffusion process with the trained surrogate model \mathcal{P}_{ϕ^*} . Standard guidance techniques (e.g., classifier-free guidance) require gradients from the guiding model. However, our surrogate \mathcal{P}_{ϕ^*} evaluates discrete graph samples, making its output non-differentiable with respect to the generator’s continuous predictions.

To overcome this, we introduce a **zero-order (ZO) optimization** step within each denoising iteration. As detailed in Algorithm 1, at each timestep t , we first use the generator \mathcal{G}_{ϕ^*} to predict the unguided clean graph, $\hat{A}_0^{(t)}$. We then sample K discrete candidate graphs from this prediction. The surrogate model \mathcal{P}_{ϕ^*} evaluates all candidates, and we se-

| Method | GSM8K | MATH | MultiArith | HumanEval | MMLU | SVAMP | Avg. |
|---------------------|-----------------------------------|-----------------------------------|-----------------------------------|-----------------------------------|-----------------------------------|-----------------------------------|-----------------------------------|
| Vanilla | 87.45 | 46.29 | 96.85 | 87.08 | 82.14 | 86.67 | 81.75 |
| CoT | 87.10 <small>↓0.35</small> | 46.40 <small>↑0.11</small> | 96.31 <small>↓0.54</small> | 88.13 <small>↑1.05</small> | 82.65 <small>↑0.51</small> | 87.33 <small>↑0.66</small> | 81.99 <small>↑0.24</small> |
| ComplexCoT | 86.89 <small>↓0.56</small> | 46.53 <small>↑0.24</small> | 96.70 <small>↓0.15</small> | 87.49 <small>↑0.41</small> | 83.78 <small>↑1.64</small> | 87.67 <small>↑1.00</small> | 81.84 <small>↑0.09</small> |
| SC (CoT \times 5) | 87.57 <small>↑0.12</small> | 47.91 <small>↑1.62</small> | 96.58 <small>↓0.27</small> | 88.60 <small>↑1.52</small> | 82.66 <small>↑0.52</small> | 88.00 <small>↑1.33</small> | 81.89 <small>↑0.14</small> |
| MultiPersona | 87.50 <small>↑0.05</small> | 45.43 <small>↓0.86</small> | 97.49 <small>↑0.64</small> | 88.32 <small>↑1.24</small> | 83.65 <small>↑1.51</small> | 87.00 <small>↑0.33</small> | 81.90 <small>↑0.15</small> |
| LLM-Debate | 89.47 <small>↑2.02</small> | 48.54 <small>↑2.25</small> | 97.33 <small>↑0.48</small> | 88.68 <small>↑1.60</small> | 83.69 <small>↑1.55</small> | 89.00 <small>↑2.33</small> | 82.79 <small>↑1.04</small> |
| LLM-Blender | 88.35 <small>↑0.90</small> | 46.92 <small>↑0.63</small> | 97.29 <small>↑0.44</small> | 88.80 <small>↑1.72</small> | 81.22 <small>↓0.92</small> | 87.33 <small>↑0.66</small> | 81.65 <small>↓0.10</small> |
| DyLAN | 89.98 <small>↑2.53</small> | 48.63 <small>↑2.34</small> | 97.12 <small>↑0.27</small> | 90.42 <small>↑3.34</small> | 80.16 <small>↓1.98</small> | 88.67 <small>↑2.00</small> | 82.50 <small>↑0.75</small> |
| AgentVerse | 89.91 <small>↑2.46</small> | 47.35 <small>↑1.06</small> | 97.50 <small>↑0.65</small> | 89.29 <small>↑2.21</small> | 81.22 <small>↓0.92</small> | 88.33 <small>↑1.66</small> | 82.27 <small>↑0.52</small> |
| MacNet | 87.95 <small>↑0.50</small> | 45.18 <small>↓1.11</small> | 96.03 <small>↓0.82</small> | 84.57 <small>↓2.51</small> | 79.85 <small>↓2.29</small> | 86.00 <small>↓0.67</small> | 79.93 <small>↓1.82</small> |
| AutoAgents | 87.69 <small>↑0.24</small> | 45.32 <small>↓0.97</small> | 96.42 <small>↓0.43</small> | 87.64 <small>↑0.56</small> | 82.13 <small>↓0.01</small> | 86.34 <small>↓0.33</small> | 80.96 <small>↓0.79</small> |
| GPTSwarm | 89.14 <small>↑1.69</small> | 47.88 <small>↑1.59</small> | 96.79 <small>↓0.06</small> | 89.32 <small>↑2.24</small> | 83.98 <small>↑1.84</small> | 88.67 <small>↑2.00</small> | 82.96 <small>↑1.21</small> |
| ADAS | 86.12 <small>↓1.33</small> | 43.18 <small>↓3.11</small> | 96.02 <small>↓0.83</small> | 84.19 <small>↓2.89</small> | 77.93 <small>↓4.21</small> | 86.33 <small>↓0.34</small> | 78.96 <small>↓2.79</small> |
| AgentSquare | 87.62 <small>↑0.17</small> | 48.51 <small>↑2.22</small> | 97.77 <small>↑0.92</small> | 89.08 <small>↑2.00</small> | 79.85 <small>↓2.29</small> | 88.00 <small>↑1.33</small> | 81.81 <small>↑0.06</small> |
| AFlow | 91.16 <small>↑3.71</small> | 51.28 <small>↑4.99</small> | 96.22 <small>↓0.63</small> | 90.93 <small>↑3.85</small> | 83.28 <small>↑1.14</small> | 88.33 <small>↑1.66</small> | 83.53 <small>↑1.78</small> |
| G-Designer | 92.09 <small>↑4.64</small> | 51.00 <small>↑4.71</small> | 97.78 <small>↑0.93</small> | 91.11 <small>↑4.03</small> | 84.50 <small>↑2.36</small> | 90.00 <small>↑3.33</small> | 84.41 <small>↑2.66</small> |
| MaAS | 92.30 <small>↑4.85</small> | 51.82 <small>↑5.53</small> | 98.80 <small>↑1.95</small> | 90.56 <small>↑3.48</small> | 83.78 <small>↑1.64</small> | 89.67 <small>↑3.00</small> | 84.49 <small>↑2.74</small> |
| GTD (Ours) | 94.14 <small>↑6.69</small> | 54.07 <small>↑7.78</small> | 98.88 <small>↑2.03</small> | 91.46 <small>↑4.38</small> | 84.58 <small>↑2.44</small> | 91.33 <small>↑4.66</small> | 85.74 <small>↑3.99</small> |

Table 1: Performance comparison on various benchmarks. All scores are accuracy (%). Changes are reported relative to the **Vanilla** baseline. The **best result** in each column is bolded. Baselines: CoT (Wei et al., 2022), ComplexCoT (Fu et al., 2022), SC (CoT \times 5) (Wang et al., 2023a), MultiPersona (Wang et al., 2023b), LLM-Debate (Du et al., 2023), LLM-Blender (Jiang et al., 2023), DyLAN (Liu et al., 2023), AgentVerse (Chen et al., 2023b), MacNet (Qian et al., 2024), AutoAgents (Chen et al., 2023a), GPTSwarm (Zhuge et al., 2024), ADAS (Hu et al., 2024b), AgentSquare (Shang et al., 2024), AFlow (Zhang et al., 2025d), G-Designer (Zhang et al., 2025a) MaAS (Zhang et al., 2025b).

5 EXPERIMENTS

To validate the effectiveness of our proposed **GTD** framework, we conduct a comprehensive set of experiments designed to evaluate its performance across three key dimensions: **(1) task-solving effectiveness**, **(2) communication cost-efficiency**, and **(3) robustness against agent failures**.

Our experimental setup is standardized across all evaluations to enable fair comparisons. The backbone for all agents is **GPT-4o-mini**. In our primary experiments, we deploy domain-specific agent teams: four **MathSolver** agents for the mathematics datasets (GSM8K, MATH, MultiArith, and SVAMP); four **CodeSolver** agents for the coding dataset (HumanEval); and three **KnowledgeableAcademic** agents for the science dataset (MMLU). The surrogate reward model (\mathcal{P}_ϕ) in the **GTD** framework is a Graph Neural Network with two GAT layers and a hidden dimension of 32, trained for 10 epochs using the Adam optimizer with mean squared error loss. The conditional diffusion generator (\mathcal{G}_θ) is a two-layer Graph Transformer with two attention heads, and the diffusion process runs for 50 timesteps. The training dataset for these models was constructed by evaluating baseline topologies on 50 samples from the GSM8K dataset. During inference, proxy-guided synthesis applies a zeroth-order optimization step, evaluating five candidate graphs at each timestep to guide the generation process.

5.1 TASK-SOLVING EFFECTIVENESS

First, we evaluated GTD’s ability to generate high-utility communication topologies by comparing its task-solving performance against a wide range of established multi-agent methods. We used several popular benchmarks for this comparison, including GSM8K, MATH, MultiArith for mathematical reasoning, and HumanEval for code generation. Baselines include canonical prompting strategies like Chain-of-Thought (CoT) (Wei et al., 2022) as well as more recent agentic frameworks such as AgentVerse (Chen et al., 2023b), AFlow (Zhang et al., 2025d), and MaAS (Zhang et al., 2025b). For each task, GTD generates a bespoke communication topology conditioned on the

problem description, and the resulting multi-agent system solves the task. Performance is measured by task-specific accuracy.

As shown in Table 1, GTD demonstrates superior performance across the majority of benchmarks. It achieves state-of-the-art results on GSM8K (94.14), MATH (54.07), MultiArith (98.88), and SVAMP (91.30), significantly outperforming all baselines. For instance, on the challenging MATH dataset, GTD improves upon the strongest baseline (MaAS) by over 2 absolute percentage points. This highlights our framework’s ability to generate highly effective, task-adaptive topologies that facilitate better collaboration among agents compared to static or heuristically-designed communication structures.

5.2 COMMUNICATION COST-EFFICIENCY

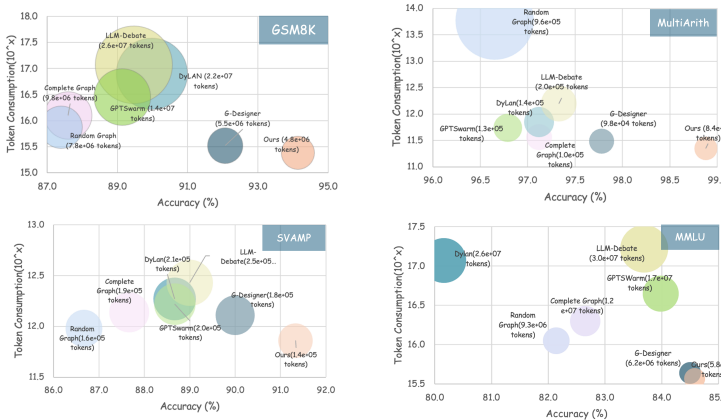


Figure 4: **Accuracy versus token consumption for various multi-agent methods across the GSM8K, MultiArith, MMLU, and SVAMP benchmarks.** The plots illustrate that topologies generated by GTD are highly cost-efficient, achieving strong performance while using significantly fewer tokens than baseline methods that rely on dense communication graphs.

the optimal bottom-right position, signifying the highest accuracy achieved with the lowest token consumption. For instance, on GSM8K, GTD achieves over 94% accuracy while consuming only 4.8e+06 tokens; in contrast, the next best performer, G-Designer, requires 15% more tokens for lower accuracy, while methods like LLM-Debate use over five times the tokens. This efficiency is even more pronounced on MultiArith, where GTD reaches nearly 99% accuracy using just 8.4e+04 tokens, setting a new Pareto frontier that no other method approaches. Similarly, on SVAMP, GTD is the only method to surpass 91% accuracy while keeping token usage at a minimum (1.4e+05 tokens). These findings show that the proxy-guided generation process successfully learns to create sparse, efficient graphs by preserving only the most critical communication links, thereby avoiding the quadratic overhead of fully-connected approaches while still enabling complex, high-performance interactions.

5.3 ROBUSTNESS AGAINST AGENT FAILURES

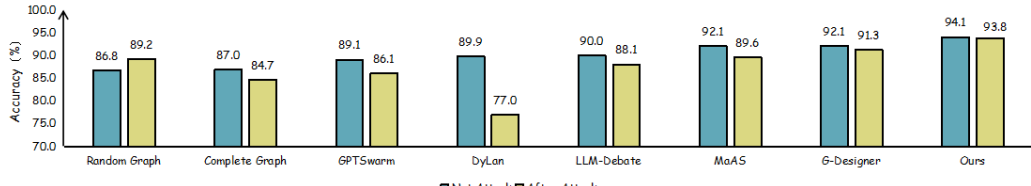


Figure 5: **Robustness of various multi-agent systems to simulated agent failure on the GSM8K benchmark.** The chart compares task accuracy before and after an attack, demonstrating that topologies generated by GTD exhibit greater resilience and more graceful performance degradation compared to other methods.

A core motivation for dynamic topology generation is to reduce unnecessary communication and minimize token consumption. Our analysis confirms that GTD generates not only effective but also significantly sparser and more cost-efficient topologies compared to methods that rely on dense or fully-connected graphs.

The results, visualized in the scatter plots in Figure 4, show GTD’s exceptional efficiency. Across all tested benchmarks: GSM8K, MultiArith, SVAMP, and MMLU. GTD consistently occupies

The structure of a communication graph critically impacts a multi-agent system’s resilience. To evaluate this, we tested the robustness of GTD-generated topologies by simulating agent failures during task execution on the GSM8K benchmark. In the experiment, a non-critical agent was randomly selected and its failure was simulated by making it produce erroneous outputs.

The results in the Figure 9 above demonstrate that GTD-generated topologies are significantly more robust to agent failure than those from all other compared methods.

While all systems experienced some performance degradation, GTD’s accuracy dropped by a mere 0.3 percentage points (from 94.1% to 93.8%), showcasing a remarkably graceful degradation. This stands in stark contrast to other methods; for instance, DyLan’s accuracy plummeted by nearly 13 points, and even a Complete Graph topology dropped by over 2 points. This experiment confirms that by jointly optimizing for multiple objectives, GTD learns to generate topologies with sufficient redundancy to bypass failed agents, ensuring high resilience in practical, imperfect scenarios.

6 ABLATION STUDIES

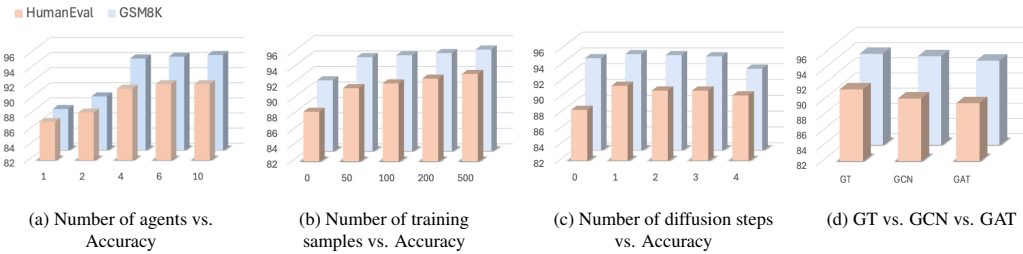


Figure 6: **Ablation studies on key hyperparameters and components of the GTD framework.** From left to right, the charts show the framework’s sensitivity to: (1) the number of agents, (2) the number of training samples, (3) the number of diffusion steps, and (4) the choice of denoising network architecture. The results consistently validate our primary design choices.

| Variant | GSM8K | HumanEval |
|-------------------|--------------|--------------|
| GTD (Ours) | 94.14 | 91.43 |
| – w/o Guidance | 88.42 | 87.19 |
| – w/ Random | 89.65 | 88.32 |

Figure 7: Ablation study on the impact of the proxy guidance mechanism.

intelligent selection offered only a minor improvement, proving that the targeted optimization is the key driver of success. Our analysis of agent team size, visualized in Figure 6 (left), revealed that performance scales effectively up to four agents but shows diminishing returns thereafter. This result validates our use of four agents as an optimal trade-off between task performance and computational efficiency. We also found the framework to be highly data-efficient, with the largest performance gains achieved within the first 50 training samples (Figure 6, second from left). This demonstrates that GTD can be trained effectively without requiring a massive, expensive dataset. Sensitivity analysis on the number of diffusion steps showed that performance peaked with a single, strong corrective step. In our architectural comparison (Figure 6, right), the Graph Transformer consistently outperformed both GCN and GAT as the denoising network. Collectively, these studies provide strong evidence that GTD’s performance stems from its specific architectural choices and its novel, data-efficient guidance mechanism.

To rigorously validate our design choices, we conducted a series of ablation studies to isolate the contribution of GTD’s core components and hyperparameters, with results summarized in Figure 6 and Figure 7. The most critical finding, shown in Figure 7, confirms the impact of our proxy-guided synthesis; removing the guidance mechanism entirely causes a performance drop of nearly 6 percentage points on GSM8K (from 94.14% to 88.42%). Furthermore, using random guidance instead of the proxy model’s

7 CONCLUSION

Existing Multi-Agent Systems (MAS) often rely on static, hand-crafted topologies that do not adapt to diverse tasks, leading to either excessive token consumption for simple problems or performance bottlenecks for complex ones. To address this, we introduce Guided Topology Diffusion (GTD), a novel generative framework that uses conditional discrete graph diffusion models to iteratively construct a communication network. Experiments show that GTD creates highly task-adaptive, sparse, and efficient topologies that significantly outperform existing methods in LLM agent collaboration and demonstrate superior robustness to agent failures.

REFERENCES

Structural topology optimisation based on a multi-agent model. <https://www.sciencedirect.com/science/article/pii/S0141029623013937>, 2023. Engineering Structures, Elsevier. Accessed 2025-08-26.

Brandon Ayal a. Topology-driven performance analyses in consensus algorithms for multi-agent systems. Master's thesis, University of Texas at Arlington, Arlington, TX, 2025. URL https://mavmatrix.uta.edu/mechaerospace_theses/1030/.

Guangyao Chen et al. Autoagents: A framework for automatic agent generation. *arXiv:2309.17288*, 2023a. URL <https://arxiv.org/abs/2309.17288>.

Sijia Chen, Xiaomin Li, Mengxue Zhang, Eric Hanchen Jiang, Qingcheng Zeng, and Chen-Hsiang Yu. Cares: Comprehensive evaluation of safety and adversarial robustness in medical llms, 2025. URL <https://arxiv.org/abs/2505.11413>.

Wenhu Chen et al. Agentverse: Facilitating multi-agent collaboration and exploring emergent behaviors. *arXiv:2308.10848*, 2023b. URL <https://arxiv.org/abs/2308.10848>.

Yao Chen, Jinhui Lü, Xinghuo Yu, and David J. Hill. Multi-agent systems with dynamical topologies: Consensus and applications. *IEEE Circuits and Systems Magazine*, 13(3):21–34, 2013. doi: 10.1109/MCAS.2013.2271443.

Dhrubajit Chowdhury and Hassan K. Khalil. Fast consensus in multi-agent systems with star topology using high gain observers. *IEEE Control Systems Letters*, 1(1):188–193, 2017.

Shifei Ding, Wei Du, Ling Ding, Lili Guo, and Jian Zhang. Learning efficient and robust multi-agent communication via graph information bottleneck. In *AAAI*, volume 38, pp. 17346–17353, 2024. doi: 10.1609/aaai.v38i16.29682. URL <https://doi.org/10.1609/aaai.v38i16.29682>.

Wei Du, Shifei Ding, Lili Guo, Jian Zhang, and Ling Ding. Expressive multi-agent communication via identity-aware learning. In *AAAI*, volume 38, pp. 17354–17361, 2024. doi: 10.1609/aaai.v38i16.29683. URL <https://doi.org/10.1609/aaai.v38i16.29683>.

Yilun Du et al. Improving factuality and reasoning in language models through multiagent debate. *arXiv:2305.14325*, 2023. URL <https://arxiv.org/abs/2305.14325>.

Yao Fu et al. Complexity-based prompting for multi-step reasoning. *arXiv:2210.00720*, 2022. URL <https://arxiv.org/abs/2210.00720>.

Ning Gong, Michael Korostelev, Qiangguo Ren, Li Bai, Saroj Biswas, and Frank Ferrese. Fault tolerant (n, k)-star power network topology for multi-agent communication in automated power distribution systems. <https://d1wqtxts1xzle7.cloudfront.net/80670305/pdf-libre.pdf>, 2015. Proceedings/Journal venue not clearly specified; accessed 2025-08-26.

Aaron Helsinger, Michael Thome, and Todd Wright. Cougaar: A scalable, distributed multi-agent architecture. In *Proceedings of the IEEE International Conference on Systems, Man and Cybernetics (SMC)*, pp. 1910–1917, The Hague, Netherlands, 2004.

Jonathan Ho and Tim Salimans. Classifier-free diffusion guidance. *arXiv:2207.12598*, 2021.

Jonathan Ho, Ajay Jain, and Pieter Abbeel. Denoising diffusion probabilistic models. In *NeurIPS*, 2020.

Sirui Hong et al. MetaGPT: Meta programming for multi-agent collaborative framework. *arXiv:2308.00352*, 2023.

Shengchao Hu, Li Shen, Ya Zhang, and Dacheng Tao. Learning multi-agent communication from graph modeling perspective. In *ICLR*, 2024a. URL <https://doi.org/10.48550/arXiv.2405.08550>.

Shunyu Hu et al. Automated design of agentic systems. *arXiv:2408.08435*, 2024b. URL <https://arxiv.org/abs/2408.08435>.

Mengda Ji, Genjiu Xu, and Liying Wang. Cora: Coalitional rational advantage decomposition for multi-agent policy gradients. *arXiv:2506.04265*, 2025. URL <https://doi.org/10.48550/arXiv.2506.04265>.

Dongfu Jiang, Bill Yuchen Lin, and Xiang Ren. LLM-Blender: Ensembling large language models with pairwise ranking and generative fusion. In *ACL*, 2023. URL <https://aclanthology.org/2023.acl-long.792/>.

Eric Hanchen Jiang, Haozheng Luo, Shengyuan Pang, Xiaomin Li, Zhenting Qi, Hengli Li, Cheng-Fu Yang, Zongyu Lin, Xinfeng Li, Hao Xu, Kai-Wei Chang, and Ying Nian Wu. Learning to rank chain-of-thought: Using a small model, 2025. URL <https://arxiv.org/abs/2505.14999>.

Guohao Li et al. CAMEL: Communicative agents for “mind” exploration with language models. *arXiv:2303.17760*, 2023.

Hengli Li, Chenxi Li, Tong Wu, Xuekai Zhu, Yuxuan Wang, Zhaoxin Yu, Eric Hanchen Jiang, Song-Chun Zhu, Zixia Jia, Ying Nian Wu, and Zilong Zheng. Seek in the dark: Reasoning via test-time instance-level policy gradient in latent space, 2025a. URL <https://arxiv.org/abs/2505.13308>.

Xiaomin Li, Xupeng Chen, Jingxuan Fan, Eric Hanchen Jiang, and Mingye Gao. Multi-head reward aggregation guided by entropy, 2025b. URL <https://arxiv.org/abs/2503.20995>.

Xinran Li, Xiaolu Wang, Chenjia Bai, and Jun Zhang. Exponential topology-enabled scalable communication in multi-agent reinforcement learning. In *ICLR*, 2025c. URL <https://arxiv.org/abs/2502.19717>.

Xiao Liang, Zhong-Zhi Li, Yeyun Gong, Yang Wang, Hengyuan Zhang, Yelong Shen, Ying Nian Wu, and Weizhu Chen. Sws: Self-aware weakness-driven problem synthesis in reinforcement learning for llm reasoning, 2025a. URL <https://arxiv.org/abs/2506.08989>.

Xiao Liang, Zhongzhi Li, Yeyun Gong, Yelong Shen, Ying Nian Wu, Zhijiang Guo, and Weizhu Chen. Beyond pass@1: Self-play with variational problem synthesis sustains rlvr, 2025b. URL <https://arxiv.org/abs/2508.14029>.

Sijia Liu et al. Zeroth-order stochastic gradient methods for nonconvex optimization. In *NeurIPS*, 2018.

Zhen Liu et al. A dynamic llm-powered agent network for task-oriented collaboration. *arXiv:2310.02170*, 2023. URL <https://arxiv.org/abs/2310.02170>.

Yat Long Lo, Biswa Sengupta, Jakob Foerster, and Michael Noukhovitch. Learning multi-agent communication with contrastive learning. *arXiv:2307.01403*, 2024. URL <https://arxiv.org/abs/2307.01403>.

Manuel Madeira, Clement Vignac, Dorina Thanou, and Pascal Frossard. Generative modelling of structurally constrained graphs. In *NeurIPS*, 2024. URL <https://arxiv.org/abs/2406.17341>.

Yurii Nesterov and Vladimir Spokoiny. Random gradient-free minimization of convex functions. *Foundations of Computational Mathematics*, 2017.

Long Ouyang et al. Training language models to follow instructions with human feedback. *arXiv:2203.02155*, 2022.

Chen Qian et al. Scaling large-language-model-based multi-agent collaboration. *arXiv:2406.07155*, 2024. URL <https://arxiv.org/abs/2406.07155>.

Yu Shang et al. Agentsquare: Automatic llm agent search in modular design space. *arXiv:2410.06153*, 2024. URL <https://arxiv.org/abs/2410.06153>.

Yang Song and Stefano Ermon. Score-based generative modeling through stochastic differential equations. In *ICLR*, 2021.

Qi Sun, Junyi Li, Zijun Yao, Shoujin Wang, Philip S. Yu, and Wenjie Zhang. Assemble your crew: Automatic multi-agent communication topology design via autoregressive graph generation. *arXiv preprint arXiv:2507.18224*, 2025. URL <https://arxiv.org/abs/2507.18224>.

Clement Vignac et al. DiGress: A generative model for graphs via diffusion. In *NeurIPS*, 2023.

Guancheng Wan, Leixin Sun, Longxu Dou, Zitong Shi, Fang Wu, Eric Hanchen Jiang, Wenke Huang, Guibin Zhang, Hejia Geng, Xiangru Tang, Zhenfei Yin, Yizhou Sun, and Wei Wang. Diagnose, localize, align: A full-stack framework for reliable llm multi-agent systems under instruction conflicts, 2025. URL <https://arxiv.org/abs/2509.23188>.

Xuezhi Wang et al. Self-consistency improves chain of thought reasoning in language models. In *ICLR*, 2023a. URL <https://arxiv.org/abs/2203.11171>.

Zhen Wang et al. Unleashing the emergent cognitive synergy of llms: A multi-persona self-collaboration framework. *arXiv:2307.05300*, 2023b. URL <https://arxiv.org/abs/2307.05300>.

Jason Wei et al. Chain-of-thought prompting elicits reasoning in large language models. *arXiv:2201.11903*, 2022. URL <https://arxiv.org/abs/2201.11903>.

Xumeng Wen, Zihan Liu, Shun Zheng, Shengyu Ye, Zhirong Wu, Yang Wang, Zhijian Xu, Xiao Liang, Junjie Li, Ziming Miao, Jiang Bian, and Mao Yang. Reinforcement learning with verifiable rewards implicitly incentivizes correct reasoning in base llms, 2025. URL <https://arxiv.org/abs/2506.14245>.

Zhenzhong Wu et al. AutoGen: Enabling next-gen LLM applications via multi-agent conversation. *arXiv:2308.08155*, 2023.

Dan Xiao and Ah-Hwee Tan. Cooperative reinforcement learning in topology-based multi-agent systems. *Autonomous Agents and Multi-Agent Systems*, 26(1):86–119, 2013. doi: 10.1007/s10458-011-9183-4.

Zhe Xu, Ruizhong Qiu, Yuzhong Chen, Huiyuan Chen, Xiran Fan, Menghai Pan, Zhichen Zeng, Mahashweta Das, and Hanghang Tong. Discrete-state continuous-time diffusion for graph generation, 2024. URL <https://arxiv.org/abs/2405.11416>.

Shijie Yang, Yihao Feng, Junning Song, Peijie Sun, Yili Wang, Chen Li, Wenjie Zhang, Shirui Pan, and Chengqi Zhang. Anymac: Cascading flexible multi-agent collaboration via next-agent prediction. *arXiv preprint arXiv:2506.17784*, 2025. URL <https://arxiv.org/abs/2506.17784>.

Jiaxuan You, Bowen Liu, Rex Ying, Vijay Pande, and Jure Leskovec. Graph convolutional policy network for goal-directed molecular graph generation. In *NeurIPS*, 2018. URL <https://doi.org/10.48550/arXiv.1806.02473>.

Tingting Yuan, Hwei-Ming Chung, Jie Yuan, and Xiaoming Fu. Dacom: Learning delay-aware communication for multi-agent reinforcement learning. In *AAAI*, 2023. URL <https://arxiv.org/abs/2212.01619>.

Guibin Zhang, Yanwei Yue, Zhixun Li, Sukwon Yun, Guancheng Wan, Kun Wang, Dawei Cheng, Jeffrey Xu Yu, and Tianlong Chen. Cut the crap: An economical communication pipeline for llm-based multi-agent systems. *arXiv preprint arXiv:2410.02506*, 2024. doi: 10.48550/arXiv.2410.02506. URL <https://arxiv.org/abs/2410.02506>. ICLR 2025 (poster), OpenReview version available.

Guibin Zhang, Yanwei Yue, Xiangguo Sun, Guancheng Wan, Miao Yu, Junfeng Fang, Kun Wang, Tianlong Chen, and Dawei Cheng. G-designer: Architecting multi-agent communication topologies via graph neural networks. *arXiv preprint arXiv:2410.11782*, 2025a. doi: 10.48550/arXiv.2410.11782. URL <https://arxiv.org/abs/2410.11782>.

Guibin Zhang et al. Multi-agent architecture search via agentic supernet. *arXiv:2502.04180*, 2025b. URL <https://arxiv.org/abs/2502.04180>.

Guochen Zhang, Aolong Zhang, Chaoli Sun, and Qing Ye. An evolutionary algorithm for multi-objective workflow scheduling with adaptive dynamic grouping. *Electronics*, 14(13):2586, 2025c. doi: 10.3390/electronics14132586. URL <https://www.mdpi.com/2079-9292/14/13/2586>.

Jiaxin Zhang et al. Aflow: Automating agentic workflow generation. In *ICLR*, 2025d. URL <https://arxiv.org/abs/2410.10762>.

Pengsong Zhang, Xiang Hu, Guowei Huang, Yang Qi, Heng Zhang, Xiuxu Li, Jiaxing Song, Jabin Luo, Yijiang Li, Shuo Yin, Chengxiao Dai, Eric Hanchen Jiang, Xiaoyan Zhou, Zhenfei Yin, Boqin Yuan, Jing Dong, Guinan Su, Guanren Qiao, Haiming Tang, Anghong Du, Lili Pan, Zhenzhong Lan, and Xinyu Liu. aixiv: A next-generation open access ecosystem for scientific discovery generated by ai scientists, 2025e. URL <https://arxiv.org/abs/2508.15126>.

Lingxiao Zhao, Xueying Ding, and Leman Akoglu. Pard: Permutation-invariant autoregressive diffusion for graph generation. In *NeurIPS*, 2024. URL <https://doi.org/10.48550/arXiv.2402.03687>.

Han Zhou, Xingchen Wan, Ruoxi Sun, Hamid Palangi, Shariq Iqbal, Ivan Vulić, Anna Korhonen, and Sercan Ö. Arik. Multi-agent design: Optimizing agents with better prompts and topologies. *arXiv preprint arXiv:2502.02533*, 2025. URL <https://arxiv.org/abs/2502.02533>.

Changxi Zhu, Mehdi Dastani, and Shihan Wang. Reducing variance caused by communication in decentralized multi-agent deep reinforcement learning, 2025. URL <https://arxiv.org/abs/2502.06261>.

Qiuming Zhu. The topologies of cooperation in knowledge intensive multi-agent systems. In *Proceedings of the IEEE International Conference on Systems, Man and Cybernetics (SMC)*, 2003. URL <https://ieeexplore.ieee.org/abstract/document/1245130>. IEEE Xplore abstract #1245130.

Qiuming Zhu. Topologies of agents interactions in knowledge intensive multi-agent systems for networked information services. *Advanced Engineering Informatics*, 20(1):31–45, 2006. doi: 10.1016/j.aei.2005.08.001. URL <https://www.sciencedirect.com/science/article/pii/S1474034605000728>.

Mingchen Zhuge et al. Language agents as optimizable graphs. *arXiv:2402.16823*, 2024. URL <https://arxiv.org/abs/2402.16823>.

A ALGORITHM

Algorithm 1 Guided Topology Diffusion (GTD) Generation

- 1: **Input:** Task condition C_{new} , trained models $\mathcal{G}_{\theta^*}, \mathcal{P}_{\phi^*}$, weights w_u, w_c .
- 2: Sample $A_T \sim \mathcal{N}(0, \mathbf{I})$.
- 3: **for** $t = T, \dots, 1$ **do**
- 4: Predict the unguided clean graph: $\hat{A}_0^{(t)} = \mathcal{G}_{\theta^*}(A_t, C_{\text{new}}, t)$.
- 5: Generate K candidates: $\{A_{0,k}^{(t)}\}_{k=1}^K$, where $A_{0,k}^{(t)} \sim \text{Bernoulli}(\text{sigmoid}(\hat{A}_0^{(t)}))$.
- 6: Evaluate candidates: For $k = 1 \dots K$, compute $[\hat{u}_k, \hat{c}_k]^T = \mathcal{P}_{\phi^*}(A_{0,k}^{(t)}, C_{\text{new}})$.
- 7: Select best candidate via ZO: $A_{0,\text{best}}^{(t)} = \arg \max_{A_{0,k}^{(t)}} (w_u \cdot \hat{u}_k - w_c \cdot \hat{c}_k)$.
- 8: Compute posterior mean μ_{post} and variance Σ_{post} for $q(A_{t-1}|A_t, A_{0,\text{best}}^{(t)})$.
- 9: Sample the next state: $A_{t-1} \sim \mathcal{N}(\mu_{\text{post}}, \Sigma_{\text{post}})$.
- 10: **end for**
- 11: **Output:** The final graph A_0 .

B DATA STATISTICS

We conclude the data statistics in the table 2.

Table 2: Dataset descriptions and statistics.

| Category | Dataset | Answer Type | Metric | #Test | License |
|-------------------|------------|--------------|--------|-------|-------------|
| General reasoning | MMLU | Multi-choice | Acc. | 1,530 | MIT License |
| | GSM8K | Number | Acc. | 1,319 | MIT License |
| | MultiArith | Number | Acc. | 180 | Unspecified |
| | SVAMP | Number | Acc. | 300 | MIT License |
| Math reasoning | Math | Number | Acc. | 500 | MIT License |
| | HumanEval | Code | Pass@1 | 164 | MIT License |

C THEORETICAL JUSTIFICATION

In this section, we provide a more formal theoretical underpinning for the GTD framework. We begin by framing the graph diffusion model within the lens of variational inference and then analyze the convergence properties of our proxy-guided synthesis process.

C.1 VARIATIONAL PERSPECTIVE OF GRAPH DIFFUSION

The generative process of denoising diffusion models can be rigorously justified as a procedure for optimizing the Evidence Lower Bound (ELBO) of the data's log-likelihood.

Definition C.1 (Evidence Lower Bound (ELBO)). *Given a data point A_0 , a joint distribution $p_{\theta}(A_{0:T}|C)$, and a variational posterior $q(A_{1:T}|A_0)$, the ELBO for the conditional log-likelihood $\log p_{\theta}(A_0|C)$ is defined as:*

$$\mathcal{L}_{\text{ELBO}} = \mathbb{E}_{q(A_{1:T}|A_0)} \left[\log \frac{p_{\theta}(A_{0:T}|C)}{q(A_{1:T}|A_0)} \right] \leq \log p_{\theta}(A_0|C) \quad (9)$$

This lower bound can be decomposed into a series of terms that are more amenable to optimization:

$$\begin{aligned} \mathcal{L}_{\text{ELBO}} &= \mathbb{E}_q [\log p_{\theta}(A_0|A_1, C)] - D_{KL}(q(A_T|A_0)||p(A_T)) \\ &\quad - \sum_{t=2}^T D_{KL}(q(A_{t-1}|A_t, A_0)||p_{\theta}(A_{t-1}|A_t, C)) \end{aligned} \quad (10)$$

Optimizing the ELBO involves minimizing the KL-divergence between the true posterior of the forward process and the learned reverse process. The forward process posterior is known to be tractable.

Lemma C.2 (Forward Process Posterior). *The posterior distribution $q(A_{t-1}|A_t, A_0)$ is a Gaussian distribution given by:*

$$q(A_{t-1}|A_t, A_0) = \mathcal{N}\left(A_{t-1}; \tilde{\mu}_t(A_t, A_0), \tilde{\beta}_t \mathbf{I}\right) \quad (11)$$

where $\tilde{\mu}_t(A_t, A_0) = \frac{\sqrt{\bar{\alpha}_{t-1}}\beta_t}{1-\bar{\alpha}_t} A_0 + \frac{\sqrt{\alpha_t}(1-\bar{\alpha}_{t-1})}{1-\bar{\alpha}_t} A_t$ and $\tilde{\beta}_t = \frac{1-\bar{\alpha}_{t-1}}{1-\bar{\alpha}_t} \beta_t$.

By parameterizing the reverse process $p_\theta(A_{t-1}|A_t, C)$ as a Gaussian whose mean is predicted by a neural network, we can connect the variational objective to a simpler, more practical training objective.

Theorem C.3 (Optimality of the Denoising Objective). *Assuming the reverse process $p_\theta(A_{t-1}|A_t, C)$ is Gaussian, minimizing the KL-divergence term $D_{KL}(q(A_{t-1}|A_t, A_0)||p_\theta(A_{t-1}|A_t, C))$ in Eq. 10 with respect to θ is equivalent to training a denoising network $\mathcal{G}_\theta(A_t, C, t)$ to predict A_0 from A_t by minimizing the L2 loss:*

$$\mathcal{L}_{\text{simple}} = \mathbb{E}_{t, A_0, C, \epsilon} \left[\|A_0 - \mathcal{G}_\theta(\sqrt{\bar{\alpha}_t} A_0 + \sqrt{1-\bar{\alpha}_t} \epsilon, C, t)\|^2 \right] \quad (12)$$

Proof. Our goal is to minimize the KL divergence between the true posterior and the learned reverse process:

$$L_t = D_{KL}(q(A_{t-1}|A_t, A_0)||p_\theta(A_{t-1}|A_t, C)) \quad (13)$$

Both distributions are Gaussian: $q(A_{t-1}|A_t, A_0) = \mathcal{N}(\cdot; \tilde{\mu}_t(A_t, A_0), \tilde{\beta}_t \mathbf{I})$ and $p_\theta(A_{t-1}|A_t, C) = \mathcal{N}(\cdot; \mu_\theta(A_t, C, t), \sigma_t^2 \mathbf{I})$. For simplicity, we fix the variance of the reverse process to match the true posterior, $\sigma_t^2 = \tilde{\beta}_t$. The KL divergence between two multivariate Gaussians $\mathcal{N}(\mu_1, \Sigma_1)$ and $\mathcal{N}(\mu_2, \Sigma_2)$ simplifies when $\Sigma_1 = \Sigma_2 = \sigma^2 \mathbf{I}$ to $\frac{1}{2\sigma^2} \|\mu_1 - \mu_2\|^2$. Therefore, minimizing the KL divergence is equivalent to minimizing the squared Euclidean distance between their means:

$$L_t = \mathbb{E}_{A_0, C, \epsilon} \left[\frac{1}{2\tilde{\beta}_t} \|\tilde{\mu}_t(A_t, A_0) - \mu_\theta(A_t, C, t)\|^2 \right] \quad (14)$$

The expression for the true posterior mean is $\tilde{\mu}_t(A_t, A_0) = \frac{\sqrt{\bar{\alpha}_{t-1}}\beta_t}{1-\bar{\alpha}_t} A_0 + \frac{\sqrt{\alpha_t}(1-\bar{\alpha}_{t-1})}{1-\bar{\alpha}_t} A_t$. We parameterize our model's mean μ_θ to have the same functional form, but predicting A_0 with our network $\mathcal{G}_\theta(A_t, C, t)$:

$$\mu_\theta(A_t, C, t) = \frac{\sqrt{\bar{\alpha}_{t-1}}\beta_t}{1-\bar{\alpha}_t} \mathcal{G}_\theta(A_t, C, t) + \frac{\sqrt{\alpha_t}(1-\bar{\alpha}_{t-1})}{1-\bar{\alpha}_t} A_t \quad (15)$$

Substituting this into the loss function, the terms involving A_t cancel out:

$$L_t = \mathbb{E}_{A_0, C, \epsilon} \left[\frac{1}{2\tilde{\beta}_t} \left\| \frac{\sqrt{\bar{\alpha}_{t-1}}\beta_t}{1-\bar{\alpha}_t} A_0 - \frac{\sqrt{\bar{\alpha}_{t-1}}\beta_t}{1-\bar{\alpha}_t} \mathcal{G}_\theta(A_t, C, t) \right\|^2 \right] \quad (16)$$

$$= \mathbb{E}_{A_0, C, \epsilon} \left[\frac{(\sqrt{\bar{\alpha}_{t-1}}\beta_t)^2}{2\tilde{\beta}_t(1-\bar{\alpha}_t)^2} \|A_0 - \mathcal{G}_\theta(A_t, C, t)\|^2 \right] \quad (17)$$

Since the term outside the norm is a positive constant for a given timestep t , minimizing L_t with respect to θ is equivalent to minimizing the simpler objective:

$$\mathcal{L}'_t = \mathbb{E}_{A_0, C, \epsilon} [\|A_0 - \mathcal{G}_\theta(A_t, C, t)\|^2] \quad (18)$$

By substituting $A_t = \sqrt{\bar{\alpha}_t} A_0 + \sqrt{1-\bar{\alpha}_t} \epsilon$ and taking the expectation over all timesteps t , we arrive at the simplified loss function $\mathcal{L}_{\text{simple}}$ stated in the theorem. \square

C.2 ANALYSIS OF PROXY-GUIDED SYNTHESIS

We now analyze the role of the surrogate model and the ZO optimization step in guiding the synthesis towards high-reward topologies.

Definition C.4 (ϵ -Accurate Surrogate Model). *A surrogate reward model \mathcal{P}_ϕ is ϵ_{\max} -accurate with respect to a true reward function $R(A, C)$ if, for any valid topology A and condition C , the approximation error is bounded:*

$$|R(A, C) - \mathcal{P}_\phi(A, C)| \leq \epsilon_{\max} \quad (19)$$

The accuracy of this model directly bounds the sub-optimality of the topology generated by an ideal proxy-guided optimizer.

Theorem C.5 (Performance Gap Bound). *Let $A^* = \arg \max_A R(A, C)$ be the true optimal topology and $A_{\text{proxy}}^* = \arg \max_A \mathcal{P}_\phi(A, C)$ be the topology found by an ideal optimizer using an ϵ_{\max} -accurate proxy. The performance gap is bounded by:*

$$R(A^*, C) - R(A_{\text{proxy}}^*, C) \leq 2\epsilon_{\max} \quad (20)$$

Proof. By definition of A_{proxy}^* as the maximizer of the proxy reward function, we have $\mathcal{P}_\phi(A_{\text{proxy}}^*, C) \geq \mathcal{P}_\phi(A^*, C)$. From the definition of an ϵ_{\max} -accurate surrogate model, we know that for any topology A , $R(A, C) \geq \mathcal{P}_\phi(A, C) - \epsilon_{\max}$. Applying this bound to A_{proxy}^* , we get:

$$R(A_{\text{proxy}}^*, C) \geq \mathcal{P}_\phi(A_{\text{proxy}}^*, C) - \epsilon_{\max} \quad (21)$$

Combining this with the optimality condition of A_{proxy}^* gives:

$$R(A_{\text{proxy}}^*, C) \geq \mathcal{P}_\phi(A^*, C) - \epsilon_{\max} \quad (22)$$

Again, from the ϵ_{\max} -accuracy definition applied to A^* , we can state that $\mathcal{P}_\phi(A^*, C) \geq R(A^*, C) - \epsilon_{\max}$. Substituting this into the previous inequality yields:

$$R(A_{\text{proxy}}^*, C) \geq (R(A^*, C) - \epsilon_{\max}) - \epsilon_{\max} \quad (23)$$

$$= R(A^*, C) - 2\epsilon_{\max} \quad (24)$$

Rearranging this final expression gives the desired bound:

$$R(A^*, C) - R(A_{\text{proxy}}^*, C) \leq 2\epsilon_{\max} \quad (25)$$

This completes the proof. \square

Corollary C.6 (Perfect Surrogate). *If the surrogate model is perfect, i.e., $\epsilon_{\max} = 0$, then any topology A_{proxy}^* that maximizes the proxy reward also maximizes the true reward, yielding $R(A_{\text{proxy}}^*, C) = R(A^*, C)$.*

Definition C.7 (ZO-Guided Denoising Step). *At a diffusion step t , given the unguided prediction $\hat{A}_0^{(t)} = \mathcal{G}_{\theta^*}(A_t, C, t)$, the ZO-guided denoising step replaces $\hat{A}_0^{(t)}$ with $A_{0,\text{best}}^{(t)}$, where:*

$$A_{0,\text{best}}^{(t)} = \arg \max_{A \in \{A_{0,k}^{(t)}\}_{k=1}^K} \mathcal{P}_\phi(A, C) \quad (26)$$

and each candidate $A_{0,k}^{(t)}$ is a discrete sample drawn from a distribution parameterized by $\hat{A}_0^{(t)}$, e.g., $A_{0,k}^{(t)} \sim \text{Bernoulli}(\sigma(\hat{A}_0^{(t)}))$.

This ZO step can be viewed as approximating a gradient ascent step on the proxy reward landscape. Let $J(\hat{A}_0) = \mathbb{E}_{A \sim p(A|\hat{A}_0)}[\mathcal{P}_\phi(A, C)]$. The true gradient $\nabla_{\hat{A}_0} J$ is intractable. The ZO step provides an update direction, $\Delta_t = A_{0,\text{best}}^{(t)} - \hat{A}_0^{(t)}$, which serves as a stochastic estimate of the ascent direction. The use of multiple samples ($K > 1$) reduces the variance of this estimate. The guided update for the next state A_{t-1} is then computed using the posterior conditioned on $A_{0,\text{best}}^{(t)}$ instead of $\hat{A}_0^{(t)}$, effectively biasing the sampling trajectory towards regions of higher proxy reward. This greedy, step-wise maximization provides a computationally efficient method for incorporating non-differentiable objectives directly into the generative process.

Table 3: The GPU cost with increasing number of agents.

| #Agents | 5 | 50 | 100 | 1000 |
|-------------|-----|-----|-----|------|
| Memory (GB) | 2.8 | 3.4 | 3.9 | 4.9 |

D SUPPLEMENTARY RESULTS

E COMPUTATIONAL RESOURCES

All experiments, including the training of the surrogate and diffusion models, as well as the multi-agent system simulations for data generation and evaluation, were conducted on a server equipped with four NVIDIA A6000 GPUs, each with 48GB of VRAM.

F ETHICS AND SOCIETAL IMPACT

This research is focused on improving the efficiency and effectiveness of multi-agent systems (MAS), which can lead to positive societal impacts like accelerating scientific discovery and reducing the energy consumption of large-scale AI computations. However, we recognize that a framework for optimizing agent coordination is a dual-use technology. In the wrong hands, it could potentially be used to orchestrate malicious activities, such as coordinating disinformation campaigns or automated attacks. Furthermore, the performance of our system is dependent on the initial dataset used to train our models; any biases present in this data could lead to the generation of suboptimal or inequitable communication structures for certain tasks. Our work is intended purely for beneficial applications, and we advocate for the establishment of strong ethical guidelines and safeguards in the development of advanced agentic systems.

G THE USE OF LARGE LANGUAGE MODELS (LLMs)

Large Language Models (LLMs) are a central component of our research methodology. The multi-agent systems evaluated in this paper are composed of agents powered by GPT-4o-mini, which perform the reasoning and communication necessary to solve complex tasks. The performance of these LLM agents is fundamental to generating our training data and evaluating the effectiveness of the communication topologies created by our GTD framework.

Separately, for the preparation of this manuscript, our use of LLMs was strictly limited to polishing the language and generating figures. All underlying research and intellectual content, including the GTD framework, its theoretical foundations, experimental design, and the analysis of results, was completed entirely by the authors.

H PROMPTS

Figure 8 presents the topologies designed by GTD under varying query difficulties for all the benchmarks.

I AGENT ROLES AND DESCRIPTIONS

Figure 9 visualizes a set of specialized agents. These roles provide diverse perspectives that are combined to produce the final answer.

| | | |
|---|---|--|
| HumanEval (case a) | HumanEval (case b) | GSM8K(case a) |
| <pre>def strlen(string: str) -> int: """ Return length of given string >>> strlen('') 0 >>> strlen('abc') 3 """</pre> | <pre>def double_the_difference(lst: List[float]) -> int: """ Given a list of numbers, return the sum of squares of the numbers in the list that are odd. Ignore numbers that are negative or not integers. If the input list is empty, return 0. """ """</pre> | <pre>{"question": "James decides to run 3 sprints 3 times a week. He runs 60 meters each sprint. How many total meters does he run a week?", "answer": "He sprints 3*3=<<3*3=9=>>9 times So he runs 9*60=<<9*60=540=>>540 meters\n\n#### 540"}</pre> |
| HumanEval (case C) | | GSM8K(case b) |
| <pre>def eat(number: int, need: int, remaining: int) -> List[int]: """ You're a hungry rabbit, and you already have eaten a certain number of carrots, but now you need to eat more carrots to complete the day's meals. You should return an array of [total number of eaten carrots after your meals, the number of carrots left after your meals] If there are not enough remaining carrots, you will eat all remaining carrots, but will still be hungry. """ """</pre> | | <pre>{"question": "There are 27 unicorns left in the world. One third of them are in the Scottish Highlands. Two thirds of the Scottish unicorns are female. How many female Scottish unicorns are there?", "answer": "Scottish\nUnicorns:27(1/3)=9\nFemale:9(2/3)=6\nunicorns\n\n#### 6"}</pre> |
| Math (case a) | MMLU (case a) | MultiArith (case a) |
| <pre>problem_data = { "problem": "If $f(x) = (3x-2)/(x-2)$, what is the value of $f(-2) + f(-1) + f(0)$? Express your answer as a common fraction.", "solution": ("f(-2) + f(-1) + f(0) = (3(-2)-2)/(-2-2) + (3(-1)-2)/(-1-2) + (3(0)-2)/(0-2) " "= (-8)/(-4) + (-5)/(-3) + (-2)/(-2) " "= 2 + 5/3 + 1 " "= 14/3"), "answer": "14/3", "subject": "Algebra", "level": 3 }</pre> | <pre>problem_data = { "question": "Find the characteristic of the ring \mathbb{Z}_2.", "subject": "abstract_algebra", "choices": ["0", "3", "12", "30"], "answer": "0" }</pre> | <pre>problem_data = { "question": "Tiffany baked 8 brownies, but needed 17 total for her party. If she used 8 cups of flour on each one, how many cups of flour does she still need?", "final_ans": "72" }</pre> |
| Math (case b) | MMLU (case b) | MultiArith (case b) |
| <pre>problem_data = { "problem": "Compute: $1-2+3-4+5-\dots+99-100$.", "solution": "(1-2) + (3-4) + \dots + (97-98) + (99-100) = 50(-1) = -50", "answer": "-50", "subject": "Intermediate Algebra", "level": 1 }</pre> | <pre>problem_data = { "question": "Which of the following is the body cavity that contains the pituitary gland?", "subject": "anatomy", "choices": ["Abdominal", "Cranial", "Pleural", "Spinal"], "answer_index": 1 }</pre> | <pre>problem_data = { "question": "Tiffany baked 8 brownies, but needed 17 total for her party. If she used 8 cups of flour on each one, how many cups of flour does she still need?", "final_ans": "72" }</pre> |
| SVAMP (case a) | | SVAMP (case a) |
| <pre>problem_data = { "ID": "chal-26", "Body": "Danny collects bottle caps and wrappers. He found 65 wrappers and 5 bottle caps at the park. Now he has 31 bottle caps and 9 wrappers in his collection.", "Question": "How many more wrappers than bottle caps did Danny find at the park?", "Equation": "(65.0 - 5.0)", "Answer": 60.0, "Type": "Subtraction" }</pre> | <pre>problem_data = { "ID": "chal-115", "Body": "Faye was placing her pencils into rows with 22 pencils in each row. She had 6 packs of pencils each one having 14 pencils.", "Question": "How many pencils does she have?", "Equation": "(6.0 * 14.0)", "Answer": 84.0, "Type": "Multiplication" }</pre> | |

Figure 8: Case study of the communication topologies designed by GTD on all benchmarks.

| | | |
|--|---|--|
|  Knowlegable Expert You are a knowlegable expert in question answering. Please give several key entities that need to be searched in wikipedia to solve the problem, for example: catfish effect, broken window effect, Shakespeare. If there is no entity in the question that needs to be searched in Wikipedia, you don't have to provide it |  Wiki Researcher You will be given a question and a wikipedia overview of the key entities within it. Please refer to them step by step to give your answer. And point out potential issues in other agent's analysis. |  Critic You are an excellent critic. Please point out potential issues in other agent's analysis point by point. |
|  Psychologist You are a psychologist. You are good at psychology, sociology, and philosophy. You give people scientific suggestions that will make them feel better. |  Historian You research and analyze cultural, economic, political, and social events in the past, collect data from primary sources and use it to develop theories about what happened during various periods of history. |  Mathematician You are a mathematician who is good at math games, arithmetic calculation, and long-term planning. |
|  Doctor You are a doctor and come up with creative treatments for illnesses or diseases. You are able to recommend conventional medicines, herbal remedies and other natural alternatives. You also consider the patient's age, lifestyle and medical history when providing your recommendations. |  Economist You are good at economics, finance, and business. You have experience on understanding charts while interpreting the macroeconomic environment prevailing across world economies. |  Lawyer You are good at law, politics, and history. |
|  Programmer You are good at computer science, engineering, and physics. You have experience in designing and developing computer software and hardware. |  Fake You are a liar who only tell lies. | |

Figure 9: Overview of the different roles in our multi-agent question answering framework. Each role represents a distinct perspective or expertise (e.g., knowledge extraction, searching, critique, mathematics, psychology, history, medicine, economics, programming, law, or deliberate deception).